



Contents lists available at ScienceDirect

# Bioorganic & Medicinal Chemistry Letters

journal homepage: [www.elsevier.com/locate/bmcl](http://www.elsevier.com/locate/bmcl)

## Design and synthesis of aminohydantoins as potent and selective human $\beta$ -secretase (BACE1) inhibitors with enhanced brain permeability

Michael S. Malamas<sup>a,\*</sup>, Albert Robichaud<sup>a,†</sup>, Jim Erdei<sup>a</sup>, Dominick Quagliato<sup>a</sup>, William Solvibile<sup>a</sup>, Ping Zhou<sup>a</sup>, Koi Morris<sup>a</sup>, Jim Turner<sup>b</sup>, Erik Wagner<sup>b</sup>, Kristi Fan<sup>b,‡</sup>, Andrea Olland<sup>c</sup>, Steve Jacobsen<sup>b,§</sup>, Peter Reinhart<sup>b,§</sup>, David Riddell<sup>b</sup>, Menelas Pangalos<sup>b,¶</sup>

<sup>a</sup> Department of Chemical Sciences, Pfizer, CN 8000, Princeton, NJ 08543-8000, USA

<sup>b</sup> Neuroscience, Pfizer, CN 8000, Princeton, NJ 08543-8000, USA

<sup>c</sup> Department of Chemical Sciences, Pfizer, 200 Cambridge Park Drive, Cambridge, MA 02140, USA

### ARTICLE INFO

#### Article history:

Received 22 July 2010

Revised 31 August 2010

Accepted 7 September 2010

Available online 15 September 2010

#### Keywords:

Alzheimer's disease (AD)

BACE1 inhibitors

beta-Amyloid peptide (A $\beta$ )

Aminohydantoins

### ABSTRACT

The identification of small molecule aminohydantoins as potent and selective human  $\beta$ -secretase inhibitors is reported. These analogs exhibit good brain permeability (40–70%), low nanomolar potency for BACE1, and demonstrate >100-fold selectivity for the structurally related aspartyl proteases cathepsin D, renin and pepsin. Alkyl and alkoxy groups at the meta-position of the P1 phenyl, which extend toward the S3 region of the enzyme, have contributed to the ligand's reduced affinity for the efflux transporter protein P-gp, and decreased topological polar surface area, thus resulting in enhanced brain permeability. A fluorine substitution at the para-position of the P1 phenyl has contributed to 100-fold decrease of CYP3A4 inhibition and enhancement of compound metabolic stability. The plasma and brain protein binding properties of these new analogs are affected by substitutions at the P1 phenyl moiety. Higher compound protein binding was observed in the brain than in the plasma. Two structurally diverse potent BACE1 inhibitors (**84** and **89**) reduced 30% plasma A $\beta$ 40 in the Tg2576 mice in vivo model at 30 mg/kg po.

© 2010 Elsevier Ltd. All rights reserved.

Alzheimer's disease (AD) is a progressive, neurodegenerative disease of the brain and is recognized as the leading cause of dementia. At the early stage, AD is associated with gradual loss of cognition that leads to complete deterioration of cognitive, and behavioral functions and ultimately death. The pathological hallmarks of AD include the extracellular deposition of  $\beta$ -amyloid peptide (A $\beta$ ), which leads to aggregation and plaque formation, and the abnormal hyperphosphorylation of tau protein, which leads to the intracellular formation of neurofibrillary tangles.<sup>1,2</sup>  $\beta$ -Amyloid deposits are predominately composed of the A $\beta$  peptides (A $\beta$ , 39–43 residues) resulting from the endoproteolysis of the amyloid precursor protein (APP).<sup>3,4</sup> Neurofibrillary tangles are intracellular aggregates of the microtubule associated protein tau.<sup>5</sup> A $\beta$  peptides result from the sequential cleavage of APP, first

at the N-terminus by  $\beta$ -secretase enzyme ( $\beta$ -site APP cleaving enzyme, BACE1<sup>||</sup>),<sup>6,1</sup> followed at the C-terminus by one or more  $\gamma$ -secretase complexes (intramembrane aspartyl proteases),<sup>7</sup> as part of the  $\beta$ -amyloidogenic pathway. During this process, two  $\beta$ -secretase cleavage products are produced; a secreted ectodomain fragment named APPsol, and the membrane bound C-terminal fragment C99 of APP. Following  $\beta$ -secretase cleavage, a second protease,  $\gamma$ -secretase, cleaves C99 to generate the toxic A $\beta$  peptides (A $\beta$ , 39–43 residues) which are secreted from the cell. Although the cause of AD remains unknown, a large body of evidence is beginning to accumulate that highlights the central role of A $\beta$  in the pathogenesis of the disease.<sup>8–11</sup> Thus, processes that limit A $\beta$  production and deposition by preventing formation, inhibiting aggregation, and/or enhancing clearance may offer effective treatments for AD. Since  $\beta$ -secretase mediated cleavage of APP is the first and rate-limiting step of the amyloidogenic possessing pathway, BACE1 inhibition is considered a prominent therapeutic target for treating AD by diminishing A $\beta$  peptide formation in AD patients.

Over the past decade, multiple groups have investigated a variety of approaches to the design of BACE1 inhibitors. These efforts

**Abbreviations:** AD, Alzheimer's disease; A $\beta$ , beta-amyloid peptide; APP,  $\beta$ -amyloid precursor protein; BACE,  $\beta$ -site APP cleaving enzyme; FRET, fluorescence resonance energy transfer; ELISA, enzyme-linked immune sandwich assay; CHO, Chinese hamster ovary.

\* Corresponding author.

E-mail address: [malamas.michael@gmail.com](mailto:malamas.michael@gmail.com) (M.S. Malamas).

<sup>†</sup> Present address: Lundbeck Research, USA.

<sup>‡</sup> Present address: Vitae Pharmaceuticals, USA.

<sup>§</sup> Present address: Proteostasis Therapeutics, USA.

<sup>¶</sup> Present address: AstraZeneca, USA.

<sup>||</sup> Atomic coordinates of the BACE1 crystal structure of compound **102** (300Z) has been deposited in the Protein Data Bank, Research Collaboratory for Structural Bioinformatics, Rutgers University, New Brunswick, New Jersey.

have produced low molecular weight BACE1 inhibitors with little or no peptidic character.<sup>12–26</sup> In addition, recent reports have revealed the application of fragment-based lead generation computational approaches as an alternate path to the design of potent small-molecule BACE1 inhibitors.<sup>27–30</sup> The discovery of low molecular weight BACE1 inhibitors has also led to the improvement of the physicochemical properties of the compounds as demonstrated by their high-permeability in cell-based assays.<sup>31a–m</sup>

While applications of computer-aided technologies and structural biology methods to design  $\beta$ -secretase inhibitors and decrease amyloid load have made significant strides, still major obstacles remain in the central delivery of these drugs, which limit their in vivo efficacy. The preclinical shortcomings of many studies are directly associated with the poor drug levels detected in the central compartments of pharmacological action. While multiple components of drug delivery can influence the drug concentration at the site of action, three major issues have impacted the poor pharmacokinetic properties of the early generations of  $\beta$ -secretase inhibitors. First, the size and polar nature of these drugs with high topological polar surface area, which influence brain permeability; second, their high susceptibility to interact with the P-glycoprotein transporter protein, which causes rapid efflux from the brain; and third their tendency to highly bind to proteins, thus limiting the free drug concentration.

We report herein the design and synthesis of new aminohydantoins as BACE1 inhibitors with improved brain permeability properties. We have previously reported<sup>32</sup> significant advancements in the design and synthesis of highly potent and selective aminohydantoins as BACE1 inhibitors, however, the preclinical in vivo efficacy of these inhibitors was rather weak. The compound properties (size, polarity, P-gp affinity) have limited the accessibility of these drugs into the central compartments (~5–10% brain permeation), affecting in the process their in vivo efficacy. The objective of this Letter is to identify and modify the structural components of the parent compound **3** (Fig. 1) that have contributed to poor brain permeability, in an effort to improve central free drug exposure and in vivo efficacy.

The compounds needed to delineate the SAR for this study were prepared according to synthetic Scheme 1. An important step for the preparation of the advanced aminohydantoins **13** (Scheme 1) was the treatment of 1,2 di-substituted diketones **12** with 1-methyl-guanidine in the presence of sodium carbonate to produce the desired products in excellent yield. Working in reverse fashion, the required diketones **12** for this transformation were prepared from acetylenes **9** upon catalytic oxidation with  $\text{PdCl}_2(\text{CH}_3\text{CN})_2$  in DMSO. In general, two routes were used for the formation of these acetylenes **9**. In route *a*, ethylenebenzenes **8** were coupled with 4-(difluoromethoxy)-1-halobenzenes **7** using the Sonogashira protocol ( $\text{PdCl}_2(\text{PPh}_3)_2$ , CuI,  $\text{Et}_3\text{N}$ , DMF). Following route *b*, 4-(difluoromethoxy)-1-halobenzenes **7** were converted to ethylenebenzenes **10a** using the Sonogashira protocol<sup>33</sup> and trimethyl-

silyl-acetylene. Brief treatment of **10a** with  $\text{Bu}_4\text{NF}$  furnished ethylenebenzenes **10b**. Coupling of ethylenebenzenes **10b** with halobenzenes **11**, as described above, produced acetylenes **9**. The required 4-(difluoromethoxy)-1-halobenzenes **7** were prepared from phenols **5** upon treatment with 2-chloro-2 difluoroacetic acid. Alkoxy analogs **15** were prepared from the corresponding phenols (**14a**,  $\text{R}_3 = \text{OH}$ ) upon treatment with alkyl halides in the presence of cesium carbonate. Acetylenes **16** were prepared from benzene bromides **14b** ( $\text{R}_3 = \text{Br}$ ) using the Sonogashira protocol and the appropriately substituted acetylenes. Alkenes **17** were prepared from benzene bromides **14b** ( $\text{R}_3 = \text{Br}$ ) by employing the Suzuki<sup>34</sup> and Stille<sup>35</sup> protocols with suitable boronates (**18**) and stannanes (**19**). All compounds described in this Letter were prepared according to Ref. 38.

With the necessary tools needed to fully investigate the SAR, the diverse array of compounds were profiled for their potency at the target enzyme, BACE1, as well as the closely related enzymes that were the focus of this investigation. The primary screening assays utilized for the program were homogenous, continuous fluorescence resonance energy transfer (FRET) protocols, representing competitive inhibition for BACE1, BACE2, cathepsin D, pepsin and renin.<sup>36</sup> The data are reported in Tables 2–6.

Cellular potency of advanced compounds was determined via a cell-based  $\text{A}\beta$  inhibition ( $\text{A}\beta 40$  or  $\text{A}\beta 42$ ) in an enzyme-linked immune sandwich assay (ELISA) in Chinese Hamster Ovary (CHO) cells, recombinantly expressing human wild-type APP (CHO-wt).

A brief summary of the previously disclosed<sup>32</sup> SAR studies of the aminohydantoins is outlined in Figure 1. The initial HTS hit **1** was optimized by using structure-based drug design techniques and exploring the S1, S2' and S3 pockets of the BACE1 enzyme. The initial SAR exploration has resulted in >3000-fold increase of the ligand's binding affinity for BACE1, and >300-fold increase in selectivity against the structurally related aspartyl proteases BACE2, cathepsin D, renin and pepsin. These initial BACE1 inhibitors **3** and **4** also demonstrated excellent cell-based potency for the BACE1 enzyme ( $\text{EC}_{50} \sim 20 \text{ nM}$ ). However, they exhibited weak efficacy in in vivo preclinical animal models studies in lowering  $\text{A}\beta$  in the brain. As reported earlier,<sup>32</sup> the ability of these compounds to reduce  $\text{A}\beta$  was evaluated in the Tg2576 mice in vivo model for lowering plasma and brain  $\text{A}\beta 40$ . While acute administration (100 mg/kg, po) of these drugs resulted in about 70% reduction of plasma  $\text{A}\beta 40$  measured at the 8 h time point ( $p < 0.001$ ), reduction of brain  $\text{A}\beta 40$  was not observed at this dose, presumably due to the limited brain exposure of the compounds. Several physicochemical parameters (size, polarity, affinity to P-gp) have affected their poor central drug exposure and in vivo efficacy. The focus of this Letter is to improve the ligand's central exposure, while maintaining the robust affinity for BACE1.

Examination of the efflux data of a representative set of aminohydantoins (Table 1) in the MDR1-MDCK permeability assay has suggested that electron rich aryl groups (pyridine, pyrimidine; entries 24, 26–27) have highly contributed to the efflux property of

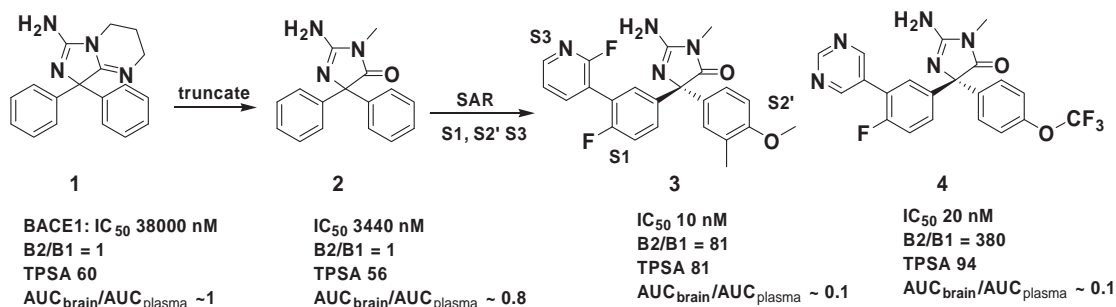
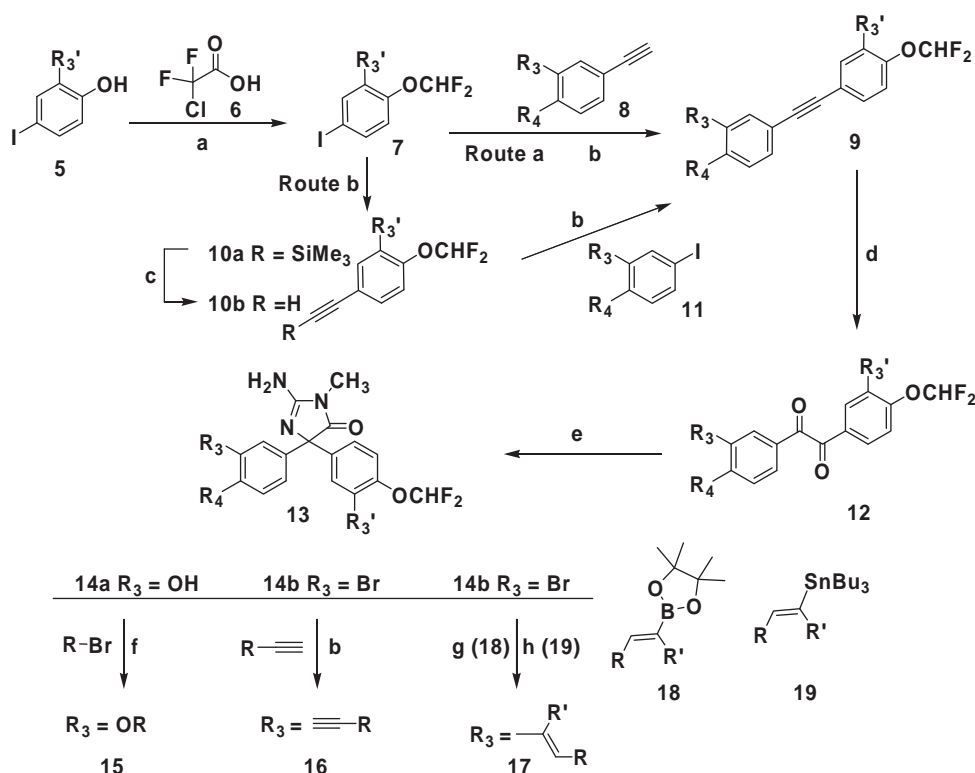
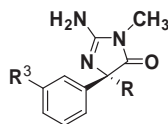


Figure 1.



**Scheme 1.** Reagents: (a)  $K_2CO_3$ , DMF; (b)  $PdCl_2(PPh_3)_2$ , CuI,  $Et_3N$ , DMF; (c)  $Bu_4NF$ , THF; (d)  $PdCl_2(CH_3CN)_2$ , DMSO; (e) 1-methylguanidine,  $Na_2CO_3$ , water, dioxane; (f)  $Cs_2CO_3$ , DMF; (g)  $Pd(PPh_3)_4$ ,  $Na_2CO_3$ , dimethoxyethane; (h)  $PdCl_2(P-tolyl)_2$ , diethoxyethane.

**Table 1**  
Aminohydantoin P-glycoprotein SAR



Compd	$R^3$	R	MDR1-MDCK BA/AB Ratio	TPSA ( $\text{\AA}^2$ )	% Brain permeability
20	H	Ph	1.2	60	81 <sup>a</sup>
21	Ph	Ph	2.2	60	—
22	2-F, 3-Pyridyl	Ph	6.8	71	—
23	Ph	3-Me,4-OMe-Ph	1.7	68	—
24	3-Pyridyl	3-Me,4-OMe-Ph	23	71	15
25	2-F, 3-Pyridyl	3-Me,4-OMe-Ph	5.5	81	10
26	2-OMe,3-Pyridyl	3-Me,4-OMe-Ph	15	88	7
27	3,5-Pyrimidine	3-Me,4-OMe-Ph	21	94	5
28	3-Pyridyl	4-OCF <sub>3</sub> -Ph	2.4	81	10
29	2-F-3-Pyridyl	4-OCF <sub>3</sub> -Ph	2.4	81	10
30	2-F, 5-F, 3-pyridyl	4-OCHF <sub>2</sub> -Ph	2.9	81	9
31	2-F, 3-pyridyl	4-OCHF <sub>2</sub> -Ph	1.7	81	9
32	H	4-OCHF <sub>2</sub> -Ph	1.9	68	90

<sup>a</sup> Ratio  $AUC_{\text{brain}}/AUC_{\text{plasma}} \times 100$ .

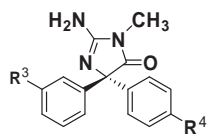
the compound. Introduction of electronegative groups (fluorine) at the P3-pyridine moiety has resulted in fourfold decrease of compound efflux (**25** vs **24**). Replacement of the pyridine group with the less electron rich phenyl moiety resulted in 13-fold reduction of compound efflux (**23** vs **24**). Additionally, the metabolically stable groups (OCF<sub>3</sub>, OCHF<sub>2</sub>; entries 28–31) at the P2' phenyl also have shown 10-fold decrease in compound efflux. The topological polar surface area (TPSA) of these analogs varied in the range of 60–94  $\text{\AA}^2$  and the brain permeability in the range of 7–90% (in vivo assessment in mice). This collection of data demonstrates that the compound's tendency to interact with P-gp and the increased TPSA values have played a critical role to the brain permeability of the compound.

For example, while analogs **28–31** showed no efflux properties, their increased TPSA values and molecular weight ( $\sim 450$ ) most likely have contributed to the low brain permeability ( $\sim 10\%$ ).

Considering the influence of the P3 substitution on P-gp affinity and increase in TPSA value, we have investigated the ligand/protein interactions at the S3 pocket of BACE1 in an attempt to design ligands with improved physicochemical properties and superior brain permeation. Our objective was to eliminate the P3 aryl group and methodically examine smaller substituents at this region. Such modifications will likely influence the ligand's physicochemical properties (P-gp, TPSA, and size) and improve brain permeability, while maintaining the robust potency for BACE1. Additionally,

**Table 2**

S2' substituted-phenyl aminohydantoin



Compd	R <sup>3</sup>	R <sup>4'</sup>	BACE1 IC <sub>50</sub> <sup>a</sup> (μM)	BACE2 IC <sub>50</sub> (μM)	Cathepsin D IC <sub>50</sub> (μM)	ELISA EC <sub>50</sub> <sup>a</sup> (μM)
<b>33</b>	2-F, 3-pyridyl	OMe	0.03	0.12	1.17	0.14
<b>34</b>	2-F, 3-pyridyl	OCF <sub>3</sub>	0.06	2.48	3.15	0.37 ± 0.08
<b>31</b>	2-F, 3-pyridyl	OCHF <sub>2</sub>	0.01 ± 0.001	0.5 ± 0.05	0.3 ± 0.01	0.027 ± 0.04
<b>35</b>	2-F, 3-pyridyl	OCH <sub>2</sub> CH <sub>2</sub> F	0.03	2.83	2.36	0.32 ± 0.2
<b>36</b>	H	OCF <sub>3</sub>	1.42 ± 0.04	2.68 ± 0.28	31.56 ± 0.84	0.81 ± 0.29
<b>32</b>	H	OCHF <sub>2</sub>	0.17 ± 0.06	1.3 ± 0.08	53 ± 9	0.16 ± 0.3
<b>37</b>	H	OCH <sub>2</sub> CH <sub>2</sub> F	1.24	11.70	116.71	2.45 ± 0.29

<sup>a</sup> IC<sub>50</sub> and EC<sub>50</sub> values are the means of at least two experiments ± SD. Values without SD are for a single determination only.

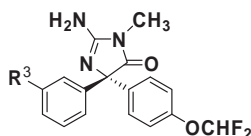
we wanted to explore electronegative groups at the P2' phenyl, which as it was shown above, have resulted in marked reduction of the compound's efflux property. To that end, replacement of the metabolically labile methoxy group of the P2' phenyl (**33**; Table 2) with various fluoro-containing alkoxy moieties (**34–37**) has produced potent analogs for BACE1. The difluoromethoxy moiety was about 10-fold more potent than the trifluoromethoxy group (**31** vs **34** and **32** vs **36**). We have used this new finding as an anchor point of our SAR exploration to identify new ligands with smaller non-aromatic P3 side chains and improved brain permeability.

Following our earlier SAR studies,<sup>32</sup> which have shown that groups at position-3 of the P1 phenyl are optimally directed toward the S3 region and increase ligand affinity, we have introduced alkyl chains at position-3 of the P1 phenyl group of **32**. A four-carbon chain analog (**40**; Table 3) showed good potency for BACE1

(IC<sub>50</sub> = 30 nM), while shorter, longer, or branched alkyl chains were less potent (**40** vs **38** and **39** & **41** and **42**). In order to improve the microsomal stability of these alkyl analogs, we have masked both the terminal carbon (prevent ω-oxidation) and the benzylic position carbon positions (entries **43–46**). Unfortunately, these modifications have produced only an incremental enhancement in the stability of the molecule. Next, we have introduced an olefinic group at the attachment point of the alkyl chain to the P1 phenyl group. The trans-isomeric analogs **47–50** were equally potent to the saturated analogs, but have shown an improvement in microsomal stability. The cis-isomer **51** was 20-fold less potent than the trans-isomer **50**. Modeling studies (not shown) have revealed that the trans-conformation of **50** allows the chain to extend deep into the S3 pocket making several hydrophobic contacts with residues of the S3 pocket, which contribute to the ligand's enhanced affinity. In contrast, the cis-isomer could not be accommodated in this

**Table 3**

Alkane and alkene substituted aminohydantoin

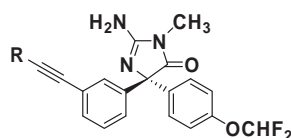


Compd	R <sup>3</sup>	BACE1 IC <sub>50</sub> <sup>a</sup> (μM)	ELISA EC <sub>50</sub> <sup>a</sup> (μM)	Microsomal stability H/R <sup>b</sup> t <sub>1/2</sub> (min)	TPSA (Å <sup>2</sup> )	MDR1-MDCK BA/AB
<b>32</b>	H	0.17 ± 0.06	0.16 ± 0.3	>30/>30	68	1.9
<b>38</b>	MeCH <sub>2</sub>	0.9	1.12 ± 0.16	9/3	68	—
<b>39</b>	Me(CH <sub>2</sub> ) <sub>2</sub>	0.09 ± 0.01	0.11 ± 0.03	3/3	68	—
<b>40</b>	Me(CH <sub>2</sub> ) <sub>3</sub>	0.03	0.1 ± 0.01	3/2	68	1.1
<b>41</b>	Me(CH <sub>2</sub> ) <sub>4</sub>	0.09	0.53 ± 0.1	5/3	68	—
<b>42</b>	MeCH <sub>2</sub> CHMeCH <sub>2</sub>	0.11	0.41 ± 0.08	4/3	68	—
<b>43</b>	CF <sub>3</sub> (CH <sub>2</sub> ) <sub>3</sub>	0.06	0.27 ± 0.08	9/6	68	1.8
<b>44</b>	CN(CH <sub>2</sub> ) <sub>3</sub>	0.05	0.09 ± 0.02	9/3	92	20
<b>45</b>	F(CH <sub>2</sub> ) <sub>3</sub> CO	0.08	0.1 ± 0.01	14/3	77	—
<b>46</b>	F(CH <sub>2</sub> ) <sub>3</sub> CHF	0.08	0.27 ± 0.08	9/3	68	—
<b>47</b>	(E)-F(CH <sub>2</sub> ) <sub>2</sub> CH=CH	0.04	0.04 ± 0.01	22/6	68	1.4
<b>48</b>	(E)-F <sub>2</sub> CHCH <sub>2</sub> CH=CH	0.03 ± 0.01	0.12 ± 0.02	26/9	68	2.3
<b>49</b>	(E)-Cyclopropyl-CH=CH	0.09	0.35 ± 0.04	25/11	68	—
<b>50</b>	(E)-Cyclopropyl-CH=CF	0.02	0.22 ± 0.06	>30/20	68	0.9
<b>51</b>	(Z)-Cyclopropyl-CH=CF	0.54	5.37 ± 0.6	5/3	68	—
<b>52</b>	(E)-MeOCH <sub>2</sub> CH=CH	0.02	0.04 ± 0.02	9/3	77	—
<b>53</b>	(E)-MeO(CH <sub>2</sub> ) <sub>2</sub> CH=CH	0.02	0.04 ± 0.01	9/6	77	—
<b>54</b>	(E)-MeO(CH <sub>2</sub> ) <sub>3</sub> CH=CH	0.05	0.1 ± 0.01	26/9	77	1.9
<b>55</b>	(E)-HO(CH <sub>2</sub> ) <sub>2</sub> CH=CH	0.05	0.1 ± 0.07	22/11	88	48
<b>56</b>	(E)-HO(CH <sub>2</sub> ) <sub>3</sub> CH=CH	0.04	0.09 ± 0.02	24/22	88	62

<sup>a</sup> IC<sub>50</sub> and EC<sub>50</sub> values are the means of at least two experiments ± SD. Values without SD are for a single determination only.<sup>b</sup> H = human, R = rat.

**Table 4**

Acetylene substituted aminohydantoins



Compd	R	BACE1 IC <sub>50</sub> <sup>a</sup> (μM)	ELISA EC <sub>50</sub> <sup>a</sup> (μM)	Microsomal stability H/R <sup>b</sup> t <sub>1/2</sub> (min)	TPSA (Å <sup>2</sup> )	MDR1-MDCK BA/AB
<b>57</b>	H	0.26	3.14 ± 0.81	29/5	68	—
<b>58</b>	Me	0.02	0.07 ± 0.02	>30/5	68	1.4
<b>59</b>	MeCH <sub>2</sub>	0.04	0.08 ± 0.02	>30/6	68	—
<b>60</b>	Me(CH <sub>2</sub> ) <sub>2</sub>	0.03 ± 0.01	0.22 ± 0.24	>30/4	68	—
<b>61</b>	FCH <sub>2</sub>	0.01	0.33 ± 0.23	>30/14	68	2.7
<b>62</b>	F(CH <sub>2</sub> ) <sub>2</sub>	0.01 ± 0.01	0.13 ± 0.14	>30/4	68	3.7
<b>63</b>	F(CH <sub>2</sub> ) <sub>4</sub>	0.04	0.07 ± 0.01	26/10	68	0.3
<b>64</b>	Me <sub>2</sub> CH	0.02	0.05 ± 0.02	26/4	68	—
<b>65</b>	Cyclopropyl	0.02	0.1 ± 0.02	>30/>30	68	2.2
<b>66</b>	Cyclohexyl	0.33	4.32 ± 0.4	>30/17	68	—
<b>67</b>	MeOCH <sub>2</sub>	0.02	0.01 ± 0.002	>30/12	77	3.8
<b>68</b>	MeO(CH <sub>2</sub> ) <sub>2</sub>	0.02 ± 0.014	0.01 ± 0.008	29/7	77	2.5
<b>69</b>	HO(CH <sub>2</sub> ) <sub>2</sub>	0.01	0.02 ± 0.004	>30/17	88	—
<b>70</b>	(R)-HOMeCH	0.02	0.07 ± 0.01	>30>30	88	37
<b>71</b>	HO(CH <sub>2</sub> ) <sub>4</sub>	0.01	0.02 ± 0.004	22/24	88	21

<sup>a</sup> IC<sub>50</sub> and EC<sub>50</sub> values are the means of at least two experiments ± SD. Values without SD are for a single determination only.<sup>b</sup> H = human, R = rat.

space very well, causing the ligand to flip upon binding, thus affecting the ligand's potency. The more polar methoxy and hydroxyl analogs (**52**–**56**) were also potent. Evaluation of the P-glycoprotein properties of these alkyl analogs in the MDR1-MDCK permeability assay revealed that all compounds minimally effluxed (Table 3), with the exception of the terminally substituted cyano- and hydroxyl-alkyls (entries **44**, **55** and **56**), which showed a pronounced efflux propensity.

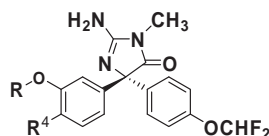
Furthermore, we have prepared analogs with the introduction of an acetylene moiety (**57**) at position-3 of the P1 phenyl (Table 4). While acetylene **57** was practically equipotent to the parent compound **32**, the methyl acetylene **58** was about 10-fold more potent than **57**, as it extends deeper into the S3 region. The longer linear analogs (**59**–**63**) were equipotent to **58**. The isopropyl and cyclopropyl groups (**64** and **65**) were also similarly potent to **58**, while the bulkier cyclohexyl group **66** was 15-fold weaker (**66** vs **65**). The linear-substituted acetylenes (Table 4) exhibited good micro-

somal stability in human microsomes, while the bulkier cyclopropyl acetylene **65** showed the best microsomal stability in both human and rodent microsomes. Evaluation of the P-glycoprotein properties of these acetylene analogs in the MDR1-MDCK permeability assay revealed that all compounds minimally effluxed (Table 4), with the exception of the hydroxyl analogs **70** and **71**, which showed strong efflux properties. Similar findings of the terminally hydroxyl substituted analogs **70** and **71** were also observed for the alkene series (entries **55** and **56**), as described above. Noteworthy is that the cell-based activity of the alkane, alkene and acetylene analogs also tracked well with their increased molecular binding, with EC<sub>50</sub> values in the range of 10–70 nM in the requisite ELISA assay.

To further expand the scope and breadth of the SAR development, the alkoxy analogs (Table 5) were prepared. The length of the alkoxy moiety was critical to the potency for BACE1. The three-carbon chain alkoxy analog **73** showed the best affinity for

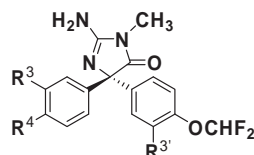
**Table 5**

Alkoxy substituted aminohydantoins

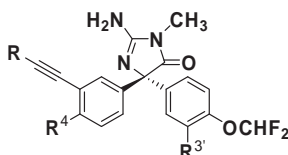


Compd	R	R <sup>4</sup>	BACE1 IC <sub>50</sub> <sup>a</sup> (μM)	ELISA EC <sub>50</sub> <sup>a</sup> (μM)	Microsomal stability H/R <sup>b</sup> t <sub>1/2</sub> (min)	MDR1-MDCK BA/AB
<b>72</b>	F(CH <sub>2</sub> ) <sub>2</sub>	F	0.12	0.4 ± 0.02	>30/10	—
<b>73</b>	F(CH <sub>2</sub> ) <sub>3</sub>	F	0.01	0.04 ± 0.01	>30/10	3.4
<b>74</b>	F(CH <sub>2</sub> ) <sub>4</sub>	F	0.1	0.15 ± 0.02	14/3	—
<b>75</b>	CF <sub>3</sub> (CH <sub>2</sub> ) <sub>2</sub>	H	0.2	1.2 ± 0.4	16/6	—
<b>76</b>	Cyclopropyl-CH <sub>2</sub>	H	0.02	0.07 ± 0.06	4/3	1.6
<b>77</b>	F <sub>2</sub> CH	H	0.2	0.3 ± 0.07	>30/>30	—
<b>78</b>	F <sub>2</sub> CHCH <sub>2</sub>	H	0.03	0.1 ± 0.02	6/5	2.2
<b>79</b>	F <sub>2</sub> CHCH <sub>2</sub>	F	0.07	0.1 ± 0.03	>30/>30	1.9
<b>80</b>	F <sub>2</sub> CH(CH <sub>2</sub> ) <sub>2</sub>	H	0.01	0.05 ± 0.01	3/3	—
<b>81</b>	F <sub>2</sub> C=CH(CH <sub>2</sub> ) <sub>2</sub>	F	0.03	0.3 ± 0.06	6/13	1.2
<b>82</b>	F <sub>2</sub> C=CH(CH <sub>2</sub> ) <sub>2</sub>	H	0.03	0.06 ± 0.02	3/5	—

<sup>a</sup> IC<sub>50</sub> and EC<sub>50</sub> values are the means of at least two experiments ± SD. Values without SD are for a single determination only.<sup>b</sup> H = human, R = rat.

**Table 6**  
Phenyl di-substituted aminohydantoin

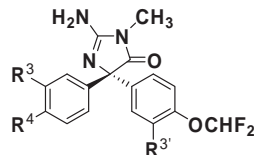
Compd	R <sup>3</sup>	R <sup>4</sup>	R <sup>3'</sup>	BACE1 IC <sub>50</sub> <sup>a</sup> (μM)	ELISA EC <sub>50</sub> <sup>a</sup> (μM)	Microsomal stability H/R <sup>b</sup> t <sub>1/2</sub> (min)	MDR1-MDCK BA/AB
<b>32</b>	H	H	H	0.17 ± 0.06	0.16 ± 0.3	>30/>30	1.9
<b>83</b>	H	H	Me	0.08	0.15 ± 0.01	>30/25	2.5
<b>84</b>	CP <sup>c</sup> -acetylene	F	H	0.02 ± 0.005	0.07 ± 0.02	>30/>30	0.8
<b>85</b>	CP-acetylene	F	Me	0.02 ± 0.01	0.09 ± 0.03	>30/>30	5.1
<b>86</b>	MeOCH <sub>2</sub> -acetylene	F	H	0.012 ± 0.004	0.03 ± 0.01	>30/10	1.6
<b>87</b>	MeOCH <sub>2</sub> -acetylene	F	Me	0.013	0.03 ± 0.01	19/5	5.6
<b>88</b>	F <sub>2</sub> CHCH <sub>2</sub> O	F	H	0.07	0.1 ± 0.03	>30/>30	1.9
<b>89</b>	F <sub>2</sub> CHCH <sub>2</sub> O	F	Me	0.015 ± 0.003	0.03 ± 0.01	>30/26	3.2

<sup>a</sup> IC<sub>50</sub> and EC<sub>50</sub> values are the means of at least two experiments ± SD. Values without SD are for a single determination only.<sup>b</sup> H = human, R = rat.<sup>c</sup> Cyclopropane.**Table 7**  
CYP3A4 inhibition of aminohydantoin

Compd		R	R <sup>3'</sup>	BACE1 IC <sub>50</sub> <sup>a</sup> (nM)		CYP3A4 IC <sub>50</sub> (μM)	
R <sup>4</sup> = H	R <sup>4</sup> = F			R <sup>4</sup> = H	R <sup>4</sup> = F	R <sup>4</sup> = H	R <sup>4</sup> = F
<b>58</b>	<b>103</b>	Me	H	22	41	<0.1	1
<b>65</b>	<b>84</b>	CP <sup>b</sup>	H	25	24 ± 5	0.1	10
<b>92</b>	<b>85</b>	CP	Me	22 ± 1	21 ± 1	0.1	4.1
<b>102</b>	<b>101</b>	<i>n</i> -Pr	Me	32	28	0.9	3.4

<sup>a</sup> IC<sub>50</sub> values are the means of at least two experiments ± SD. Values without SD are for a single determination only.<sup>b</sup> Cyclopropane.

BACE1 (IC<sub>50</sub> = 10 nM), while either shorter or longer alkoxy versions (**72** and **74**) were about 10-fold less potent. The terminal trifluoromethyl analog **75** was about 20-fold weaker than the analogous mono-fluoro analog **73**. Unfavorable electrostatic interactions between ligand **75** and the protein may have impacted its potency, considering the increased electronegative potential of the trifluoromethyl group. Next, we focused on the stability of the alkoxy analogs. The short-chained alkoxy analogs were metabolically more stable than the analogous longer-chained counterparts (**72**, **73** vs **74**). The difluoromethoxy analog **77** was the most stable compound in both human and rodent microsomes, while the one-carbon longer analog **78** was highly unstable. Introduction of a fluorine atom at position-4 of the P1 phenyl (entry **79**) has resulted in a remarkable enhancement in stability of compound **79** (**79** vs **78**). The difluoro-alkene analogs **81** and **82** were also potent for BACE1, but not very stable. Several alkoxy analogs were evaluated in the MDR1-MDCK permeability assay and showed no efflux properties.

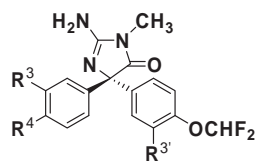
**Table 8**  
Protein binding properties of aminohydantoin

Compd	R <sup>3</sup>	R <sup>4</sup>	R <sup>3'</sup>	C log P	% Fraction unbound drug <sup>a</sup> rat SD @ 10 μM	
					Plasma	Brain
<b>32</b>	H	H	H	2.21	10.7	2.4
<b>95</b>	H	H	Me	2.71	5.6	0.9
<b>96</b>	FCH <sub>2</sub> -AC <sup>b</sup>	F	H	2.42	1.6	0.4
<b>61</b>	FCH <sub>2</sub> -AC	H	H	2.28	1.7	0.6
<b>97</b>	FCH <sub>2</sub> -AC	F	Me	2.92	0.82	0.18
<b>98</b>	FCH <sub>2</sub> -AC	H	Me	2.78	2.75	0.34
<b>86</b>	MeOCH <sub>2</sub> -AC	F	H	1.88	1.9	0.6
<b>87</b>	MeOCH <sub>2</sub> -AC	F	Me	2.38	1.4	0.3
<b>84</b>	Cyclopropyl-AC	F	H	3.59	0.7	0.07
<b>99</b>	F <sub>2</sub> CHCH <sub>2</sub> O	F	Me	3.29	3.7	0.7
<b>100</b>	F <sub>2</sub> CH(CH <sub>2</sub> ) <sub>2</sub> O	F	Me	2.41	1.6	0.6

<sup>a</sup> Dialysis was performed using 200 μL plasma versus 200 μL PBS buffer and 200 μL brain homogenates versus PBS buffer for 5 h.<sup>b</sup> Acetylene.



**Table 9**  
Phenyl di-substituted aminohydantoin



Compd	R <sup>3</sup>	R <sup>4</sup>	R <sup>3'</sup>	BACE1 IC <sub>50</sub> <sup>a</sup> (μM)	BACE2 IC <sub>50</sub> <sup>a</sup> (μM)	Cathepsin D IC <sub>50</sub> <sup>a</sup> (μM)	Pepsin % inhibition @ 100 μM	Renin IC <sub>50</sub> <sup>a</sup> (μM)
<b>32</b>	H	H	H	0.17 ± 0.06	0.26 ± 0.02	53.3 ± 9	7	44 ± 4
<b>95</b>	H	H	Me	0.08	0.85	22.5	7	38% @100 uM
<b>58</b>	Me-AC <sup>b</sup>	H	H	0.02	0.21	4.12	7	5.6
<b>60</b>	Me(CH <sub>2</sub> ) <sub>2</sub> -AC	H	H	0.03 ± 0.01	0.35 ± 0.04	4.2 ± 0.5	9	5.9
<b>63</b>	F(CH <sub>2</sub> ) <sub>3</sub> -AC	H	H	0.02 ± 0.001	0.32 ± 0.04	3.5 ± 1.4	7	6.1
<b>102</b>	F(CH <sub>2</sub> ) <sub>3</sub> -AC	F	H	0.014	0.4	1.15	5	5.9
<b>97</b>	FCH <sub>2</sub> -AC	F	Me	0.02	0.17	2.2	9	16.6
<b>67</b>	MeOCH <sub>2</sub> -AC	H	H	0.02	0.14	6.2	2	5.3
<b>68</b>	MeO(CH <sub>2</sub> ) <sub>2</sub> -AC	H	H	0.02 ± 0.014	0.1	9.9 ± 1.5	8	8.1
<b>64</b>	Me <sub>2</sub> CH-AC	H	H	0.02	0.04	4.8	9	10.9
<b>65</b>	Cyclopropyl-AC	H	H	0.02	0.07	3.75	8	7.7
<b>84</b>	Cyclopropyl-AC	F	H	0.02 ± 0.005	0.12	1.5	20	4.8
<b>92</b>	Cyclopropyl-AC	H	Me	0.02 ± 0.006	0.05	2.0	19	8.6
<b>85</b>	Cyclopropyl-AC	F	Me	0.02 ± 0.001	0.16	1.8 ± 0.2	24	6.0
<b>101</b>	Me(CH <sub>2</sub> ) <sub>2</sub> -AC	F	Me	0.03	0.11	2.12	23	16.9
<b>73</b>	F(CH <sub>2</sub> ) <sub>3</sub> O-	F	H	0.01	0.28	2.98	12	6.9
<b>79</b>	F <sub>2</sub> CHCH <sub>2</sub> O	F	H	0.07	0.73	2.6	10	8.6
<b>89</b>	F <sub>2</sub> CHCH <sub>2</sub> O	F	Me	0.015 ± 0.003	0.37 ± 0.06	3.4 ± 0.17	7	30.1

<sup>a</sup> IC<sub>50</sub> and EC<sub>50</sub> values are the means of at least two experiments ± SD. Values without SD are for a single determination only.

<sup>b</sup> Acetylene.

Next, we have examined the effect of substitution at position-3' of the phenyl moiety located at the S2' pocket (Table 6). Earlier studies<sup>32</sup> have shown that a methyl group at this position has enhanced the ligand potency about 2–3-fold (**32** vs **83**). We have selected three representative compounds (**84**, **86** and **88**) from the SAR studies described above, and have introduced a methyl substitution at position-3' of the P2' phenyl (Table 6). The binding affinity of the methyl-substituted acetylenes **85** and **87** was similar to that of the parent compounds **84** and **86**, respectively, while a fourfold potency improvement was observed for the alkoxy analog **89** (**88** vs **89**). Examining the efflux properties of these new analogs, we have noticed that while the alkoxy analogs have maintained similar efflux properties, the acetylene substituted methyl analogs **85** and **87** showed an about fivefold increase in compound efflux compared to the unsubstituted counterparts.

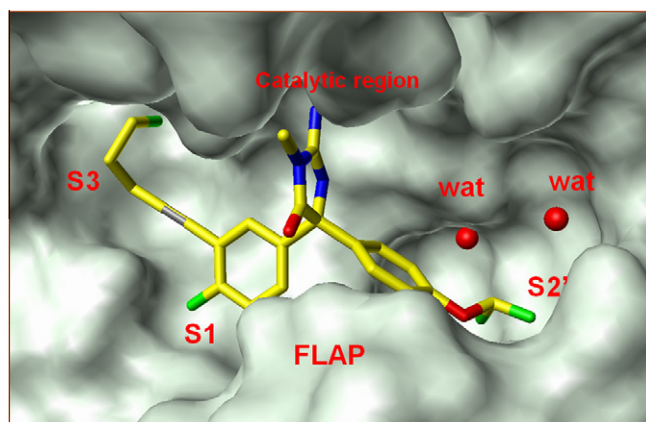


**Figure 2.** Crystal structure of BACE1 complexed with **102** shown in yellow. Substituents at the meta-position of the P1 phenyl project deep into S3 pocket and displace the buried water at the S3 region. The difluoromethoxy of P2' occupies the S2' region and interacts with the two conserved waters. The aminohydantoin portion of the ligand orients toward the catalytic region of the enzyme and interacts with the catalytic aspartic acids Asp32 and Asp228 (not shown).

Furthermore, we have concentrated our efforts to address and refine the cytochrome P450 metabolism of the P1 phenyl observed with the acetylene analogs. We have discovered that introduction of a fluorine atom at position-4 of the P1 phenyl has minimized the CYP3A4 oxidation by about 40–100-fold. A representative set of supporting data are shown in Table 7. Larger groups at this position are not favored, since they markedly reduce the compound potency, as we have reported in earlier studies.<sup>32</sup>

Considerable attention was also directed to the compound's protein binding property. Table 8 shows the effects on plasma and brain protein binding relative to the ligand's substitution pattern, where substitutions at the P1 and P2' phenyls have affected the protein binding property of these new analogs. Acetylene analogs shown in Table 8 have exhibited a 10-fold increase in plasma and brain protein binding compared to the parent compound **32**. Examining the lipophilic character of these new analogs, we have observed only a modest correlation between lipophilicity and brain permeability. For example, compounds **32** and **61** with identical C log P values, they differ fivefold in both plasma and brain protein binding values. The P1 phenyl alkoxy analogs **99** and **100** have shown 2–3× lower tendency to bind to proteins than the acetylene analogs. Methyl substitution at the P2' phenyl has resulted in two-fold increase in plasma and brain protein binding (**95** vs **32**). Interestingly, the compound protein binding levels appear to be about 5–10-fold higher in the brain than in the plasma (Table 8). This protein binding difference between plasma and brain, which affects the free drug level of the compound at the site of biological action, may explain the greater in vivo efficacy of this class of compounds to lower A<sub>β40</sub> in plasma than in brain.

In support of our modeling studies and design of BACE1 ligands, compound **102** was cocrystallized with the BACE1 enzyme (Fig. 2). The acetylene group at the meta-position of the P1 phenyl projects deep into S3 pocket and displaces the buried water at the S3 region. The difluoromethoxy moiety at the P2' phenyl occupies the S2' region and interacts with the two conserved waters (fluorine-water hydrogen-bonding interactions). The aminohydantoin portion of the ligand orients toward the catalytic region of the enzyme

and interacts with the catalytic aspartic acids Asp32 and Asp228 (not shown).

To confirm the specificity of the aminohydantoin for the BACE1 enzyme, a representative set of compounds was evaluated for inhibition of the closely related cathepsin D, renin and pepsin aspartyl proteases. As shown in Table 9, all compounds demonstrated weak inhibition for these targets.

The brain permeability of several compounds was assessed in vivo by comparing the pharmacokinetic AUC values in brain and plasma. All tested compounds showed higher brain permeability than the earlier disclosed BACE1 inhibitors. The brain permeation of the new analogs ranged between 40–70% versus 5–10% for the previous analogs. To further elucidate the ability of these ligands to reduce A $\beta$ , two structurally diverse compounds **84** and **89** were evaluated in the Tg2576 mice in vivo model for lowering plasma and brain A $\beta$ 40.<sup>37</sup> Acute administration of these inhibitors at 30 mg/kg po resulted in a significant 25–30% reduction of plasma A $\beta$ 40 measured at the 8 h time point ( $p < 0.001$ ). Significant reduction of brain A $\beta$ 40 was not observed at this dose. While these new inhibitors have shown an increase in brain permeability (40–70%), the unexpected 10-fold enhancement in brain protein binding, relatively to the plasma levels, has resulted in a low central free drug exposure, thus diminishing the A $\beta$ 40 lowering in the brain.

In this Letter, we have described a detailed and stepwise exploration of the S3 region of BACE1 by replacing the aryl group of the parent aminohydantoin **3** with various alkyl and alkoxy chains. These new analogs have exhibited better brain permeability, low nanomolar potency for BACE1, and >100-fold selectivity for the other structurally related aspartyl proteases cathepsin D, renin and pepsin. Our design strategy followed a traditional SAR approach and was supported by molecular modeling studies based on the previously reported aminohydantoin **3**.<sup>32</sup> The new inhibitors have shown decreased susceptibility to P-glycoprotein transporter protein, as demonstrated by the marked reduction of the compound's efflux property, lower topological polar surface area, and reduced molecular weight. These improved physicochemical properties have resulted in the enhancement of the compound's brain permeability level (~40–70%). We have identified that a fluorine substitution at the para-position of the P1 phenyl has dramatically decreased the cytochrome P450 metabolism and also has contributed to the metabolic stability of the alkoxy analogs. Substitutions at the P1 and P2' phenyl moieties have affected the plasma and brain protein binding levels of these new analogs, with the brain protein binding levels being 5–10-fold higher than the plasma levels. Two structurally diverse potent BACE1 inhibitors (**84** and **89**) reduced 25–30% plasma A $\beta$ 40 in the Tg2576 mice in vivo model at 30 mg/kg po.

## References and notes

- Dickson, D. W. *J. Neuropathol. Exp. Neurol.* **1997**, *56*, 321.
- Selkoe, D. J. *Science* **1997**, *275*, 630.
- Vassar, R.; Citron, M. *Neuron* **2000**, *27*, 416.
- Selkoe, D. J. *Physiol. Rev.* **2001**, *81*, 741.
- Selkoe, D. J. *Ann. Int. Med.* **2004**, *140*, 627.
- Arendt, T. *Neuroscience* **2001**, *102*, 723.
- Hardy, J.; Selkoe, D. J. *Science* **2002**, *297*, 353.
- Selkoe, D. *Ann. N.Y. Acad. Sci.* **2000**, *924*, 17.
- Coughlan, C.; Breen, K. C. *Pharm. Ther.* **2000**, *86*, 111.
- Racchi, M.; Govone, S. *Trends Pharmacol. Sci.* **1999**, *20*, 418.
- Checler, F. J. *Neurochem.* **1995**, *65*, 1431.
- Ghosh, A.; Kumaragurubaran, N.; Tang, J. *Curr. Top. Med. Chem.* **2005**, *5*, 1609.
- Cumming, J. N.; Iserloh, U.; Kennedy, M. E. *Curr. Opin. Drug Discov. Dev.* **2004**, *7*, 536.
- Durham, T. B.; Shepherd, T. A. *Curr. Opin. Drug Discov. Dev.* **2006**, *9*, 776.
- Baxter, E. W.; Reitz, A. B. *Ann. Rep. Med. Chem.* **2005**, *40*, 35.
- Schmidt, B.; Baumann, S.; Braub, H. A.; Larbig, G. *Curr. Top. Med. Chem.* **2006**, *6*, 377.
- Guo, T.; Hobbs, D. W. *Curr. Med. Chem.* **2006**, *13*, 1811.
- John, V.; Beck, J. P.; Bienkowski, M. J.; Sinha, S.; Heinrikson, R. J. *Med. Chem.* **2003**, *46*, 4625.
- Carmen Villaverde, M.; Gonzalez-Louro, L.; Sussman, F. *Curr. Top. Med. Chem.* **2007**, *7*, 980.
- Hong, L.; Koelsch, L.; Lin, X.; Wu, S.; Terzyan, S.; Ghosh, A.; Zhang, X. C.; Tang, J. *Science* **2000**, *290*, 150.
- Stachel, S. J.; Coburn, C. A.; Steele, T. G.; Jones, K. G.; Loutzenhiser, E. F.; Grego, A. R.; Rajapakse, H. A.; Lai, M.-T.; Crouthamel, M.-C.; Xu, M.; Tugusheva, K.; Lineberger, J. E.; Pietrak, B. L.; Espeseth, A. S.; Shi, X.-P.; Chen-Dodson, E.; Holloway, M. K.; Munshi, S.; Simon, A. J.; Kuo, L.; Vacca, J. P. *J. Med. Chem.* **2004**, *47*, 6447.
- Coburn, C. A.; Stachel, S. J.; Li, Y.-M.; Rush, D. M.; Steele, T. G.; Chen-Dodson, E.; Holloway, M. K.; Xu, M.; Huang, Q.; Lai, M.-T.; DiMuzio, J.; Crouthamel, M.-C.; Shi, X.-P.; Sardana, V.; Chen, Z.; Munshi, S.; Kuo, L.; Makara, G. M.; Annis, D. A.; Tadikonda, P. K.; Nash, H. M.; Vacca, J. P. *J. Med. Chem.* **2004**, *47*, 6117.
- Garino, C.; Pietrancosta, N.; Laras, Y.; Moret, V.; Rolland, A.; Quelever, G.; Kraus, J.-L. *Bioorg. Med. Chem. Lett.* **2006**, *16*, 1995.
- Huang, D.; Luthi, U.; Kolb, P.; Cecchine, M.; Barberis, A.; Caffisch, A. *J. Am. Chem. Soc.* **2006**, *128*, 5436.
- Huang, D.; Luthi, U.; Kolb, P.; Adler, K.; Cecchine, M.; Audedat, S.; Barberis, A.; Caffisch, A. *J. Med. Chem.* **2005**, *48*, 5108.
- Rajapakse, H. A.; Nantermet, P. G.; Selnick, H. G.; Munshi, S.; McGaughey, G. B.; Lindsley, S. R.; Young, M. B.; Lai, M.-T.; Espeseth, A. S.; Shi, X.-P.; Colussi, D.; Pietrak, B.; Crouthamel, M.-C.; Tugusheva, K.; Huang, Q.; Simon, A. J.; Kuo, L.; Hazuda, D. J.; Graham, S.; Vacca, J. P. *J. Med. Chem.* **2006**, *49*, 7270.
- Edwards, P. D.; Albert, J. S.; Sylvester, M.; Aharon, D.; Andisik, D.; Callaghan, O.; Campbell, J. B.; Carr, R. A.; Chessari, G.; Congreve, M.; Frederickson, M.; Folmer, R. H.; Geschwindner, S.; Koether, G.; Kolmodin, K.; Krumrine, J.; Mauger, R. C.; Murray, C. W.; Olsson, L.; Patel, S.; Spear, N.; Tian, G. *J. Med. Chem.* **2007**, *50*, 5912.
- Murray, C. W.; Callaghan, O.; Chessari, A.; Congreve, M.; Frederickson, M.; Hartshorn, M. J.; McMenamin, R.; Patel, S.; Wallis, N. *J. Med. Chem.* **2007**, *50*, 1116.
- (a) Congreve, M.; Aharon, D.; Albert, J.; Callaghan, O.; Campbell, J.; Carr, R. A.; Chessari, G.; Cowan, S.; Edwards, P. D.; Frederickson, M.; McMenamin, R.; Murray, C. W.; Patel, S.; Wallis, N. *J. Med. Chem.* **2007**, *50*, 1124; (b) Zhu, Z.; Sun, Z.; Ye, Y.; Voigt, J.; Strickland, C.; Smith, E.; Cumming, J.; Wang, L.; Wong, J.; Wang, Y.; Wyss, D.; Chen, X.; Kuvelkar, R.; Kennedy, M.; Favreau, L.; Parker, E.; McKittrick, B.; Stamford, A.; Czarniecki, M.; Greenlee, W.; Hunter, J. *J. Med. Chem.* **2010**, *53*, 951.
- Geschwindner, S.; Olsson, L.-L.; Albert, J.; Deinum, J.; Edwards, P. D.; de Beer, T.; Folmer, R. H. *A. J. Med. Chem.* **2007**, *50*, 5903.
- (a) Stanton, M.; Stauffer, S.; Grego, A.; Steinbeiser, M.; Nantermet, P.; Sankaranarayanan, S.; Price, E.; Wu, G.; Crouthamel, M.-C.; Ellis, J.; Lai, M.-T.; Espeseth, A.; Shi, X.-P.; Jin, L.; Colussi, D.; Pietrak, B.; Huang, Q.; Xu, M.; Simon, A.; Graham, S.; Vacca, J.; Selnick, H. *J. Med. Chem.* **2007**, *50*, 3431; (b) Baxter, E.; Conway, K.; Kennis, L.; Bischoff, F.; Mercken, M.; De Winter, H.; Reynolds, C.; Tounge, B.; Cuo, C.; Scott, M.; Huang, Y.; Braeken, M.; Pieters, S.; Berthelot, D.; Masure, S.; W. Bruinzeel, W.; Jordan, A.; Parker, M.; Boyd, R.; Qu, J.; Alexander, R.; Brennen, D.; Reitz, A. *J. Med. Chem.* **2007**, *50*, 4261; (c) Charrier, N.; Clarke, B.; Cutler, L.; Demont, E.; Dingwall, C.; Dunsdon, R.; East, P.; Hawkins, J.; Howes, C.; Hussain, I.; Jeffrey, P.; Maile, G.; Matico, R.; Mosley, J.; Naylor, A.; O'Brien, A.; Redshaw, S.; Rowland, P.; Soleil, V.; KSmith, K.; Sweitzer, S.; PTheobald, P.; Vesey, D.; Walter, D.; Wayne, G. *J. Med. Chem.* **2008**, *51*, 3313; (d) Iserloh, U.; Wu, Y.; Cumming, J. N.; Pan, J.; Wang, L. Y.; Stamford, A. W.; Kennedy, M. E.; Kuvelkar, R.; Chen, X.; Parker, E. M.; Strickland, C.; Voigt, J. *Bioorg. Med. Chem. Lett.* **2008**, *18*, 414; (e) Iserloh, U.; Pan, J.; Stamford, A. W.; Kennedy, M. E.; Zhang, Q.; Zhang, L.; Parker, E. M.; Mchugh, N. A.; Favreau, L.; Strickland, C.; Voigt, J. *Bioorg. Med. Chem. Lett.* **2008**, *18*, 418; (f) Clarke, B.; Demont, E.; Dingwall, C.; Dunsdon, R.; Faller, A.; Hawkins, J.; Hussain, I.; Maile, G.; Matico, R.; Mosley, J.; Milner, P.; Mosley, J.; Naylor, A.; O'Brien, A.; Redshaw, S.; Riddell, D.; Rowland, P.; Soleil, V.; Smith, K.; Stanway, S. *Bioorg. Med. Chem. Lett.* **2008**, *18*, 1017; (g) Beswick, P.; Charrier, N.; Clarke, B.; Demont, E.; Dingwall, C.; Dunsdon, R.; Faller, A.; Gleave, R.; Hawkins, J.; Hussain, I.; Johnson, C.; MacPherson, D.; Maile, G.; Matico, R.; Milner, P.; Mosley, J.; Naylor, A.; O'Brien, A.; Redshaw, S.; Riddell, D.; Rowland, P.; Skidmore, J.; VSoleil, V.; Smith, K. J.; Stanway, S.; Stemp, G.; Stuart, A.; Sweitzer, S.; Theobald, P.; Vesey, D.; Walter, D.; Ward, J.; Wayne, G. *Bioorg. Med. Chem. Lett.* **2008**, *18*, 1022; (h) Heuisil Park, H.; Kyeongsik Min, K.; Hyo-Shin Kwak, H.-S.; Ki Dong Koo, K.; Dongchul Lim, D.; Sang-Won Seo, S.-W.; Jae-Ung Choi, J.-U.; Bettina Platt, B.; Deog-Young Choi, D.-Y. *Bioorg. Med. Chem. Lett.* **2008**, *18*, 2900; (i) Cumming, J. N.; Le, T.; Babu, S.; Carroll, C.; Chen, X.; Favreau, L.; Gaspari, P.; Guo, T.; Hobbs, D.; Huang, Y.; Iserloh, U.; Kennedy, M.; Kuvelkar, R.; Li, G.; Lowrie, J.; McHugh, N.; Ozgur, L.; JPan, J.; Parker, E.; Saionz, K.; Stamford, A.; Strickland, C.; Tadesse, D.; Voigt, J.; Wang, L.; Wu, Y.; Zhang, L.; Zhang, Q. *Bioorg. Med. Chem. Lett.* **2008**, *18*, 3236; (j) Charrier, N.; Clarke, B.; Cutler, L.; Demont, E.; Dingwall, C.; Dunsdon, R.; Hawkins, J.; Howes, C.; Hubbard, J.; Hussain, I.; Maile, G.; Matico, R.; Mosley, J.; Naylor, A.; O'Brien, A.; Redshaw, S.; Rowland, P.; Soleil, V.; Smith, K.; Sweitzer, S.; Theobald, P.; Vesey, D.; Walter, D.; Wayne, G. *Bioorg. Med. Chem. Lett.* **2009**, *19*, 3664; (k) Charrier, N.; Clarke, B.; Demont, E.; Dingwall, C.; Dunsdon, R.; Hawkins, J.; Hubbard, J.; Hussain, I.; Maile, G.; Matico, R.; Mosley, J.; Naylor, A.; O'Brien, A.; Redshaw, S.; Rowland, P.; Soleil, V.; Smith, K.; Sweitzer, S.; Theobald, P.; Vesey, D.; Walter, D.; Wayne, G. *Bioorg. Med. Chem. Lett.* **2009**, *19*, 3669; (l) Charrier, N.; Clarke, B.; Cutler, L.; Demont, E.; Dingwall, C.; Dunsdon, R.; Hawkins, J.; Howes, C.; Hubbard, J.; Hussain, I.; Maile, G.; Matico, R.; Mosley, J.; Naylor, A.; O'Brien, A.; Redshaw, S.



- Rowland, P.; Soleil, V.; Smith, K.; Sweitzer, S.; Theobald, P.; Vesey, D.; Walter, D.; Wayne, G. *Bioorg. Med. Chem. Lett.* **2009**, *19*, 3674; (m) Barrow, J.; Rittle, K.; Ngo, P.; Selnick, H.; Graham, S.; Pitzenberger, S.; McGaughey, G.; Colussi, D.; Lai, M.-T.; Huang, Q.; Tugusheva, K.; Espeseth, A.; Simon, A.; Munshi, S.; Vacca, J. *ChemMedChem* **2007**, *2*, 995.
32. (a) Malamas, M. S.; Erdei, J.; Gunawan, I.; Turner, J.; Hu, Y.; Wagner, E.; Fan, K.; Chopra, R.; Olland, A.; Bard, J.; Jacobsen, S.; Magolda, R.; Pangalos, M.; Robichaud, A. J. *J. Med. Chem.* **2010**, *53*, 1146; (b) Malamas, M. S.; Barnes, K.; Johnson, M.; Hui, Y.; Zhou, P.; Turner, J.; Hu, Y.; Wagner, E.; Fan, K.; Chopra, R.; Olland, A.; Bard, J.; Pangalos, M.; Reinhart, P.; Robichaud, A. J. *Bioorg. Med. Chem.* **2010**, *18*, 630; (c) Malamas, M. S.; Erdei, J.; Gunawan, I.; Barnes, K.; Johnson, M.; Hui, Y.; Turner, J.; Hu, Y.; Erik Wagner, E.; Kristi Fan, K.; Olland, A.; Bard, J.; Robichaud, A. J. *J. Med. Chem.* **2009**, *52*, 6314.
33. Sonogashira, K.; Tohda, Y.; Hagihara, N. *Tetrahedron Lett.* **1975**, *50*, 4467.
34. Miyaoura, N.; Suzuki, A. *Chem. Rev.* **1995**, *95*, 2457.
35. Stille, J. K. *Angew. Chem., Int. Ed. Engl.* **1986**, *25*, 508.
36. Wu, P.; Brand, L. *Anal. Biochem.* **1994**, *218*, 1.
37. Hsiao, K.; Chapman, P.; Nilsen, S.; Eckman, C.; Harigaya, Y.; Younkin, S.; Yang, F.; Cole, G. *Science* **1996**, *274*, 99.
38. Detailed experimental protocols of the compounds described in this paper are reported in WO 115552, 2008; WO 118379, 2008; U.S. Patent 7423158, 2008; U.S. Patent 7723368, 2010.